22

Enzymology and Life at the Single Molecule Level

X. Sunney Xie

Summary. The advent of room-temperature single-molecule imaging and spectroscopy in the early 1990s made it possible to follow biochemical reactions and conformational dynamics of an individual enzyme molecule in real time, yielding new information about the working of enzymes *in vitro*. This eventually led to the recent success of probing single-molecule biochemical reactions in a living cell with high specificity, millisecond time resolution, and nanometer spatial precision. We have studied how gene expression and regulation occur at the single-molecule level in living bacterial cells. The examples herein illustrate the impact of the single-molecule approach on biological discovery, as well as prospects for medicine.

22.1 Introduction

Advances in life sciences in the last half-century, from the discovery of DNA structure to the crystal structure of enzymes, have been facilitated by the development of physical tools, such as X-ray crystallography. We face new challenges in understanding how the enzymes work in real time, how they work individually, how they work together in a living cell, and how the different genes get turned on and off in a living cell.

At the start of my independent career in the early 1990s, I was very fortunate to be able to participate in the development of single-molecule imaging and spectroscopy at room temperature, which was prompted by prior success under cryogenic conditions [1, 2]. The room-temperature work was initially accomplished with near-field microscopes [3–5], then much more easily with far-field fluorescence microscopes [6, 7]. As recognized in 1976 [8], the key idea behind single-molecule detection at room temperature was to use a microscope to reduce an excitation volume in order to suppress the background signal [9, 10]. In my opinion, these developments on room-temperature detection, imaging and spectroscopy of single-molecules with a far-field microscope, together with the then emerging single-molecule manipulation techniques [11–13], opened the exciting possibility of studying a large

variety of single-molecule behaviors in biology, beyond single ion channel recording [14].

As the methodologies were being developed and refined, the challenge, both technical and intellectual, was how to create a new science with new tools at the boundaries of physics, chemistry and biology. The application of single-molecule imaging, spectroscopy and manipulation to biology has led to widespread research activities around the world, which have made an impact on biochemistry and molecular biology. This is primarily because many compelling problems in biology can best be addressed with the single-molecule approach.

My group's first step in biochemistry was to monitor the biochemical reactions and conformational dynamics of a single enzyme molecule in real time by fluorescence detection [15]. Thanks to the development of *in vitro* assays, single-molecule enzymology has since provided mechanistic understanding of specific systems, as well as fundamental insights into enzymatic catalysis, and even the prospect of human genome sequencing by single-molecule methods.

The utility of single-molecule studies in biology is best illustrated by the fact that in a living cell there are only one or two copies of a particular gene on the chromosome DNA, at which fundamental biological processes such as gene expression and regulation take place. Consequently, these processes occur stochastically, and are intrinsically asynchronous among different cells. Hence, understanding of these processes requires real-time observations with single-molecule sensitivity. In 2006, we developed strategies to study these processes at the single-molecule level in living cells [16, 17]. Since then, it has been a revelation to see quantitative understanding of these processes emerging from these studies.

Below I summarize my group's work in single-molecule enzymology and gene expression and regulation in living bacteria, with a commentary on the future of single-molecule studies in biology and medicine.

22.2 Single Molecule Enzymology: The Fluctuating Enzyme

Essential to all life processes, enzymes are biological catalysts that accelerate biochemical reactions with high efficiency and high fidelity, unmatched by artificial systems. Despite more and more structures and interaction networks of enzymes becoming known, the quest for understanding how an enzyme works in real time at the molecular level remains a vital question.

In 1998, we reported the real-time observation of enzymatic turnovers of a single-molecule cholesterol oxidase, a flavoenzyme that catalyzes oxidation of cholesterol by oxygen [15] (Fig. 22.1A). The active site of the enzyme, flavin adenine dinucleotide (FAD), (Fig. 22.1B), is naturally fluorescent in its oxidized form but not in its reduced form. With excess amounts of cholesterol

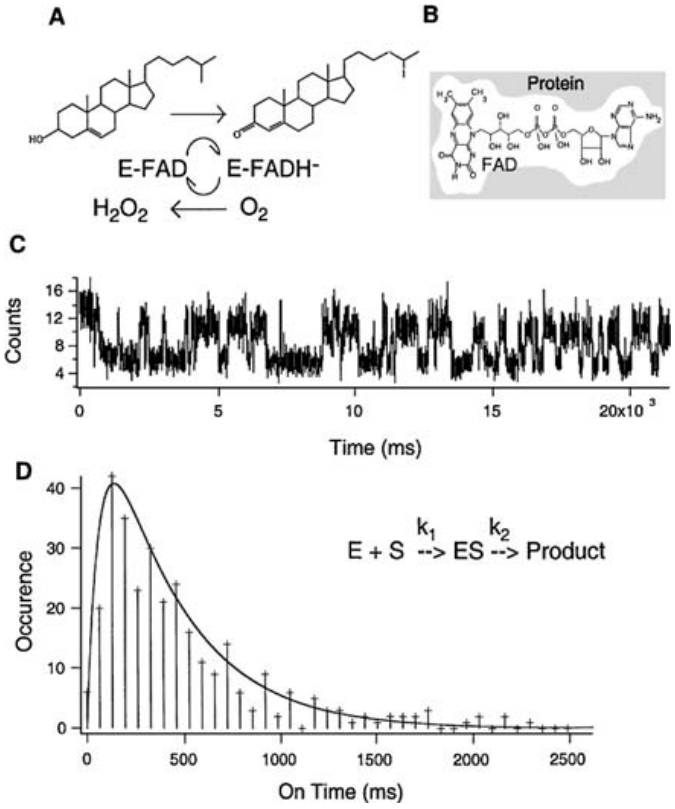

Fig. 22.1. (**A**) Enzymatic cycle of cholesterol oxidase which catalyzes the oxidation of cholesterol by oxygen. The enzyme's naturally fluorescent FAD active site is first reduced by a cholesterol substrate molecule, generating a non-fluorescent $FADH_2$, which is then oxidized by oxygen. (**B**) Structure of FAD, the active site of cholesterol oxidase. (**C**) A portion of the fluorescence intensity time trace of a single cholesterol oxidase molecule. Each on-off cycle of emission corresponds to an enzymatic turnover. (**D**) Distribution of emission on-times derived from (C). The solid line is the convolution of two exponential functions with rate constants $k_1[\mathrm{S}] = 2.5\,\mathrm{s}^{-1}$ and $k_2 = 15.3\,\mathrm{s}^{-1}$, reflecting the existence of an intermediate, ES, the enzyme–substrate complex, as shown in the kinetic scheme in the inset. From ref. [15]

and oxygen, the emission from a single enzyme molecule confined in an agarose gel exhibits an on-off behavior (Fig. 22.1C), each on-off cycle corresponding to an enzymatic turnover. The exponential rise and decay of the histogram of the waiting times indicate the existence of the enzyme–substrate complex (Fig. 22.1D).

By conducting statistical analyses of the data, we found that a single enzyme molecule exhibits fluctuations of catalytic rates – a single enzyme molecule does not have a rate constant! This phenomenon, which had been hidden in the conventional experiments, turned out to be general.

We attributed the rate constant fluctuation to conformational interconversion, which had been inferred by Frauenfelder and co-workers in their earlier work on photolysis of heme proteins [18]. We developed a method that made

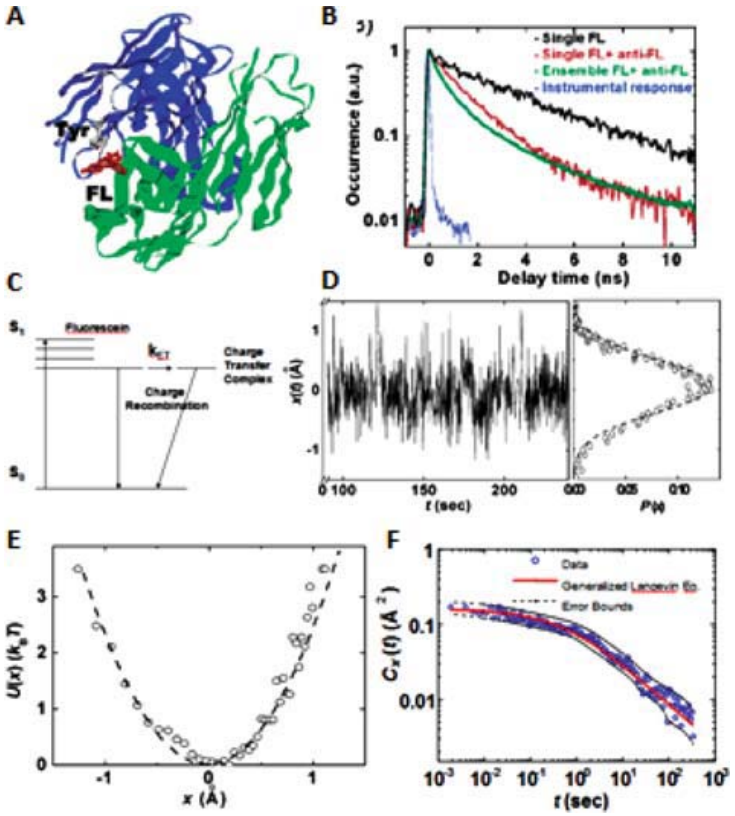

Fig. 22.2. (**A**) Fluorescein (FL) and anti-FL complex with the electron transfer donor and acceptor, Tyr37 and FL, respectively. (**B**) Monoexponential fluorescence lifetime decay for a single FL molecule (*black curve*), multiexponential fluorescence decay for the FL/anti-FL complex at both ensemble (*green curve*) and single-molecule (*red curve*) levels, and the instrumental response function (*blue curve*). (**C**) Energy diagram of the ground and excited states of fluorescein and the charge transfer state. (**D**) A segment of the donor–acceptor distance, $x(t)$ trajectory with the corresponding probability density function $P(x)$ with a Gaussian fit. (**E**) Harmonic potential of mean force, $U(x) = -k_{\mathrm{B}}T\ \ln[P(x)]$. (**F**) Autocorrelation of the donor–acceptor distance in (E) that shows the broad range of time scale distance fluctuation. From ref. [20]

it possible to directly observe conformational changes of an individual protein (e.g., Fig. 22.2A and B). [19,20] This was accomplished by using electron transfer as a distance-dependent probe (Fig. 22.2C) [19], which is complementary to fluorescent resonant energy transfer (FRET) [21], but is capable of probing angstrom scale distance fluctuation in an intact protein (Fig. 22.2A). The distance between an electron transfer donor and an acceptor was found to take place at a broad range of time scales, ranging from 10 ms to 10 s (Fig. 22.2D–F)

This equilibrium conformational fluctuation is again a general phenomenon that occurs in every system that we have studied, taking place at the same time scales at which we observed the enzymatic rate fluctuations. Such

conformational fluctuations at a broad range of time scales result from the flexible but glassy nature of enzymes as biopolymers, yet interestingly exhibit a large effect in the rates of enzymatic reactions.

Like enzymology in general, single-molecule enzymology is primarily limited by assay developments. Here, I list the single-molecule enzymatic turnover assays by fluorescence detection using

1. A fluorescent active site, as described for cholesterol oxidase
2. Fluorescently labeled substrate molecules, such as ATP or dNTP, which require either low substrate concentrations [22] or zero-mode waveguide to suppress [23]
3. FRET pair that reports conformational changes triggered by enzymes, such as staphylococcal nuclease [24], a ribozyme [25], T4 Lysozyme [26]
4. Intensity change of a fluorophore that is associated with conformational change induced by a DNA polymerase [27]
5. Fluorogenic substrate molecules that produce fluorescent product molecules by enzymatic reactions, as proposed for horseradish peroxidase [28]. Because fluorophores are continuously replenished and diffuse away from the excitation volume, this assay circumvents the photobleaching problem that hampers all the other assays, and provides extremely long time traces [29, 30]

Most ensemble enzymatic kinetics have been satisfactorily described by the classic Michaelis-Menten equation [31]. The observation of conformational dynamics occurring on multiple time scales raises an intriguing question: why does the Michaelis-Menten equation work so well despite the broad distributions and dynamic fluctuations at the single-molecule level?

We conducted a single-molecule experiment on β-galactosidase with a fluorogenic substrate that offers superb statistics (Fig. 22.3). This study allowed us to confirm the dispersed kinetics (Fig. 22.3C) and fluctuations of the catalytic rate at multiple time scales, from 10 ms to 10 s (Fig. 22.3D). Interestingly, despite the fluctuations, the Michaelis-Menten equation still holds on a single enzyme basis, except k_{cat} and K_{m} bear different microscopic interpretations, i.e., the weighted average of different conformers [29].

This explains why the Michaelis-Menten equation works so well even in the presence of large fluctuations at a broad range of time scales. This intrinsic fluctuation is not significant for a system that comprises a large number of enzyme molecules; knowing the ensemble, the average result would be sufficient. However, if, in a living cell, there is only one or a few copies of a particular enzyme, these fluctuations may result in a large physiological effect.

It is important to stress that single-molecule enzyme turnover experiments are distinctly different from conventional *in vitro* enzymatic assays in that they are conducted under a nonequilibrium steady state condition with invariant substrate concentrations [32, 33], which is the usual condition in a living cell.

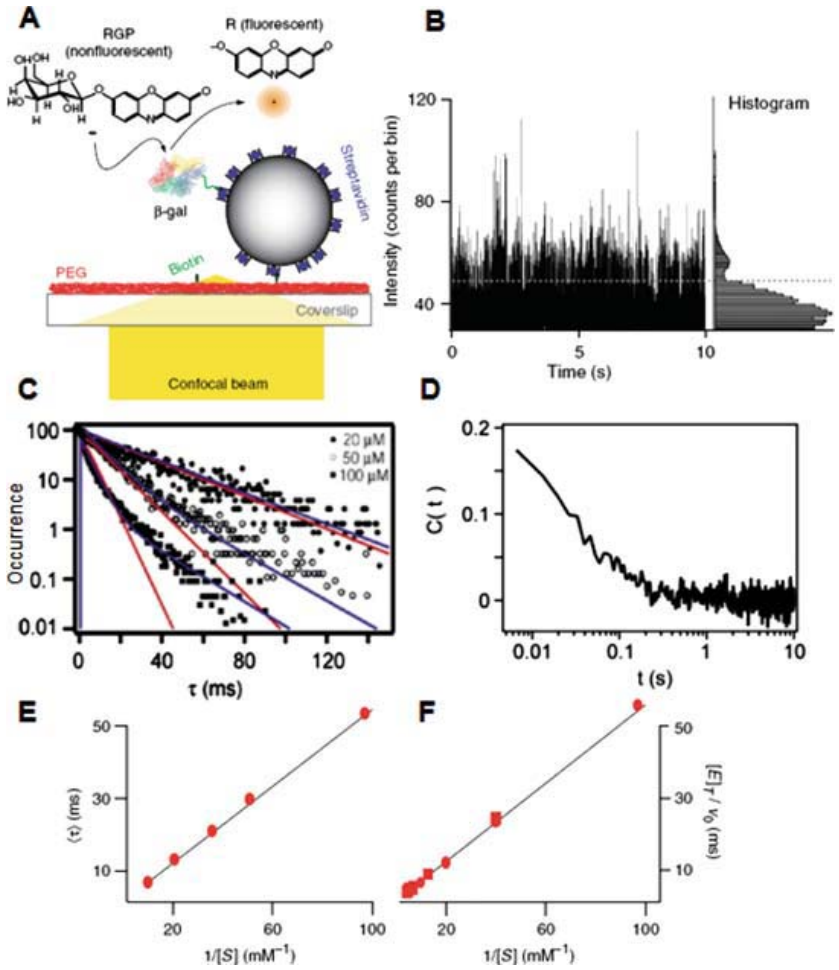

Fig. 22.3. (**A**) One β-galactosidase enzyme molecule is linked to a streptavidin-coated polystyrene bead via a flexible PEG linker. The bead binds to the biotin-PEG surface of a cover slip. The hydrolysis of the photogenic substrate RGP is catalyzed by an enzyme, and the fluorescent product resorufin (R) is monitored in the diffraction-limited confocal volume. (**B**) A segment of the chronological waiting time trajectory as a function of time. (**C**) Histograms of the waiting time distributions at different substrate concentrations [S]. (**D**) Normalized autocorrelation functions of waiting times in the time trace in (B). This highlights the broad range of time scales of turnover rate fluctuations, spanning at least four decades from 10^{-3} to 10 s. (**E**) Single-molecule Lineweaver-Burke plot of mean waiting times vs. 1/[S]. (**F**) Ensemble averaged Lineweaver-Burke plot agrees well with (E), indicating that the Michaelis-Menten equation holds on a single-molecule basis despite the fluctuation. From ref. [29].

22.3 Gene Expression and Regulation in Bacteria: Life at the Single-Molecule Level

A compelling challenge is conducting single-molecule experiments in a living cell. We have developed two strategies for studying DNA protein interactions at the single-molecule level: detection by localization and stroboscopic

illumination, which allow probing of individual fluorescent protein molecules (FP) with specific labels in millisecond time resolution and nanometer spatial precision [34]. Prior to our work, tandem repeats of FPs had been used to monitor single mRNA molecules in live cells [35, 36]. We have used our single FP sensitivity to study a variety of fundamental processes in molecular biology.

Gene expression is a single-molecule problem because most genes often exist in one or two copies per cell. In 2008, we reported the first direct observation of the production of protein molecules as they are generated one at a time, in a single live *E. coli* cell, yielding quantitative information about gene expression [16, 17] (Fig. 22.4). Under the repressed condition, protein molecules are produced in bursts (Fig. 22.4B), with each burst originating from a stochastically-transcribed single messenger RNA (mRNA) molecule; the protein copy numbers in a burst follow an exponential distribution (Fig. 22.4D), as was previously predicted theoretically [37].

Gene expression is regulated by transcription factors (TFs), which bind to specific sequences on chromosomal DNA, called operators, in controlling the transcription by RNA polymerase. We made the first real-time observation of binding and dissociation of a TF on chromosome DNA in a live cell with the method of detection by localization [38]. The *lac* repressor was fused with a yellow fluorescent protein, and monitored in response to the addition and dilution of an inducer, a lactose analog [34]. At high inducer concentration, upon inducer binding within a few seconds, the *lac* repressor dissociates from the *lac* operators (Fig. 22.5A). After a sudden dilution of extracellular inducer concentration by a factor of 50, the rebinding of a *lac* repressor to the operators takes 60 s (Fig. 22.5B). It had been previously deduced from indirect experiments that a *lac* repressor molecule finds an operator through a combined 1D diffusion along DNA and 3D diffusion through cytoplasm (Fig. 22.6A) [39]. Using the method of stroboscopic illumination (Fig. 22.6B and C), we proved quantitatively that during the ∼60 s search time for the operator in the *E. coli* genome, a *lac* repressor spends ∼90% of its time non-specifically bound to and diffusing along DNA with a residence time of ∼ 5 ms (Fig. 22.6D).

We then studied the gene regulation of the lactose metabolism in *E. coli* using the classic *lac* operon [40] which includes the *lacZ* and *lacY* genes encoding β-galactosidase and lactose permease, respectively [41] (Fig. 22.7A). β-galactosidase catalyzes the hydrolysis of lactose, whereas lactose permease is a membrane channel for lactose to enter the cell. Expression of the *lac* operon is regulated by the *lac* repressor. Under high extracellular concentrations of inducers, e.g., methyl-β-D-thiogalactoside (TMG), the dissociation of the *lac* repressor from the operators allows transcription; the *lac* genes are fully expressed for every cell in a population. However, at moderate inducer concentrations, the *lac* genes are highly expressed in only a fraction of a population, which allows the entire *E. coli* population to conserve resources in the environment. Thus, genetically identical cells in the same environment can exhibit different phenotypes. A single cell's decision on the phenotype

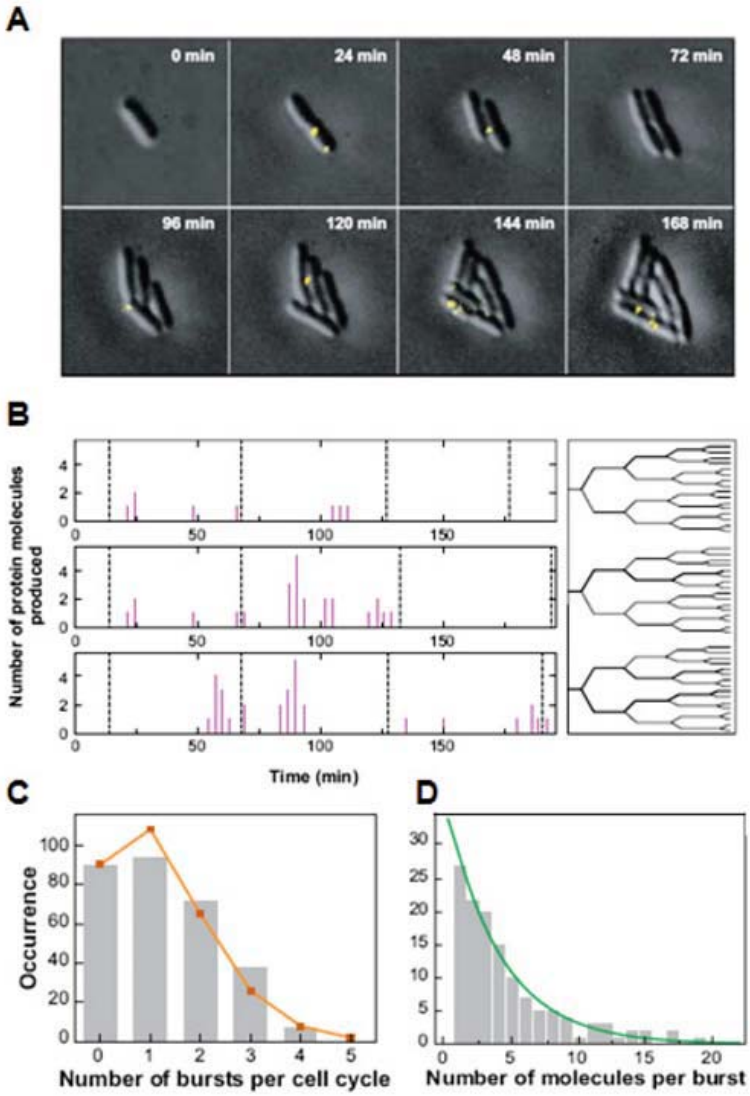

Fig. 22.4. (**A**) Time-lapse movie of fluorescence images (*yellow*) overlaid with simultaneous DIC images (*gray*) of *E. coli* cells expressing a membrane protein fused with YFP under the repressed condition. Each yellow spot is due to one YFP generated by gene expression. (**B**) Time traces of the expression of YFP molecules (*left*) along three particular cell lineages (*right*). The vertical axis is the number of protein molecules newly synthesized during the last 3 min. The dotted lines mark the cell division times. Protein production occurs in stochastic bursts, each due to one copy of mRNA and generates variable numbers of YFP molecules. (**C**) Histogram of the number of expression bursts per cell cycle. The fit is a Poisson distribution of an average of 1.2 mRNA per cell cycle. (**D**) Distribution of the number of YFPs in each gene expression burst, which follows an exponential distribution with an average of four molecules per burst. From ref. [16]

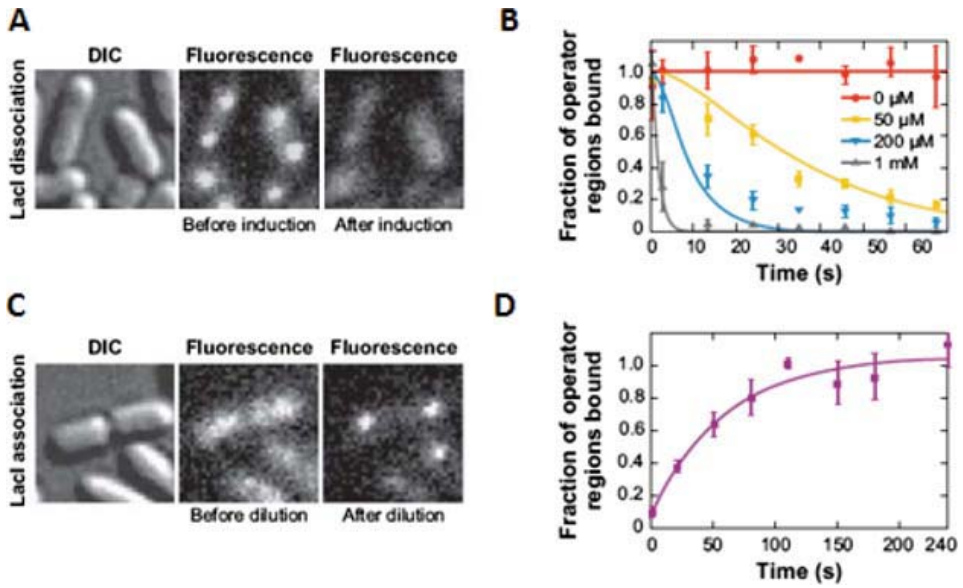

Fig. 22.5. (**A**) *E. coli* cells with YFP-labeled *lac* repressor before and 40 s after addition of inducer IPTG to a final concentration of 1 mM. (**B**) Fraction of *lac* operons in a cell population bound to repressors is plotted as a function of time after adding various concentrations of IPTG. (**C**) *E. coli* cells with YFP-labeled *lac* repressor before and 1 min after rapid dilution of IPTG from 100 to 2 mM. (**D**) Fraction of the operator region that is bound to the repressor as a function of time after the rapid dilution of inducer concentration by factor of 50. The rebinding times are exponentially fitted with a time constant of 60 s. From ref. [38]

to be exhibited is made by the bistable genetic switch, the *lac* operon. We investigated the molecular mechanism that controls the phenotype switching of a single cell.

We labeled the lactose permease with a yellow fluorescent protein. The two specific phenotypes under discussion are: first, above a certain threshold number of the permease, a cell has a fluorescent membrane and is capable of lactose metabolism; second below this threshold, a cell is non-fluorescent and is incapable of lactose metabolism. The two phenotypes coexist in a population of cells (Fig. 22.7B) and show a bimodal distribution (Fig. 22.7C). This threshold is determined to be ∼300, corresponding to a big burst of permease production.

The *lac* repressor is a tetramer that can simultaneously bind to two operators to form a DNA loop and dissociates from DNA under a high inducer concentration [38] (Fig. 22.8A). Under low inducer concentrations (Fig. 22.8B), the repressor cannot be pulled off the DNA by the inducer. Rather, spontaneously, partial dissociations of the repressor result in transcription of one mRNA and a small burst of proteins, as seen in Fig. 22.4B. However, infrequent events of complete dissociation of the repressor result in large bursts of permease expression that trigger induction of the *lac* operon

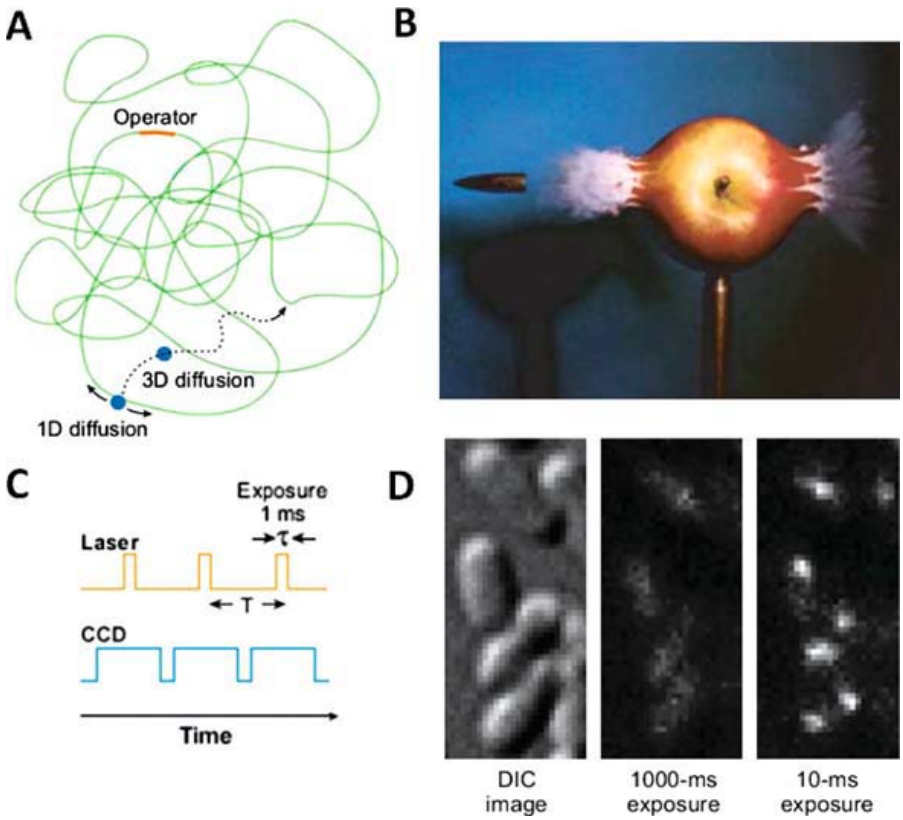

Fig. 22.6. (**A**) In searching for a target DNA sequence, a DNA repressor first non-specifically binds to DNA and undergoes 1D diffusion along a short segment of DNA before dissociating from DNA, diffusing in 3D through the cytoplasm, and rebinding to a different DNA segment. (**B**) Image of a bullet passing through an apple. From the Harold and Esther Edgerton Foundation. (**C**) Timing diagram for stroboscopic illumination. Each laser pulse is synchronized to a CCD frame that lasts for time T. (**D**) Two fluorescence images with different exposure times and the corresponding DIC image of the IPTG-induced *E. coli* cells. At 1 s, individual *lac* repressor-Venus molecules appear as diffuse fluorescence background. At 10 ms, they are clearly visible as nearly diffraction-limited spots. This indicates that the residence time of repressor is ∼10 ms. From ref. [38]

(Fig. 22.8C). We now understand the working of the bistable genetic switch at the molecular level [41].

This study proves that the stochastic single-molecule event of complete dissociation of the tetrameric *lac* repressor from DNA is solely responsible for the life changing decision of the cell, switching from one phenotype to another. This finding highlights the importance of single-molecule behaviors in biology [41].

22.4 In the Future

Single-molecule enzymology has yielded new information about how macromolecular machines work *in vitro*. No doubt we have so much left to learn; the field will be active for many years to come.

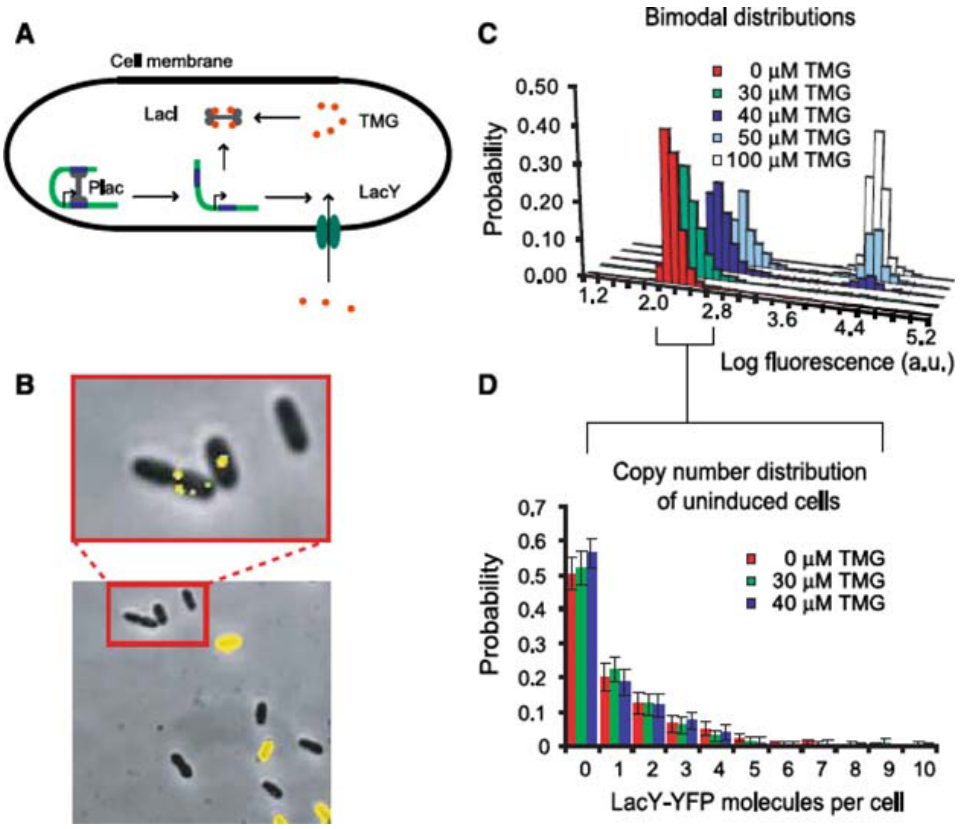

Fig. 22.7. (**A**) Gene expression of lactose permease in *E. coli*. Expression of permease *Lac* I increases the intracellular concentration of the inducer TMG, which causes the dissociation of *Lac*I from the promoter, leading to even more expression of permeases. (**B**) Cells expressing a *Lac*Y-YFP fusion exhibit all-or-none fluorescence in a fluorescence-phase contrast overlay (bottom, image dimensions 31 μm × 31 μm). Cells with a sufficient number of permeases are fully induced, whereas cells with too few permeases will stay uninduced. Fluorescence imaging with high sensitivity reveals single molecules of permease in the uninduced cells (top, image dimensions 8 μm × 13 μm). (**C**) Bimodal fluorescence distributions show that a fraction of the population exists either in an uninduced or induced state, with the relative fractions depending on the TMG concentration. (**D**) The distributions of *Lac*Y-YFP molecules in the uninduced fraction of the bimodal population at different TMG concentrations, measured with single-molecule sensitivity, indicate that one permease molecule is not enough to induce the *lac* operon. From ref. [41]

Meanwhile, an ultimate application of single-molecule enzymology that might have a societal impact is DNA sequencing, i.e., the real-time monitoring of a DNA polymerase that continuously replicates a single strand DNA template by incorporating different dye-labeled dNTPs. Currently, two commercial single-molecule sequencers have been developed [42, 43]. While others, including my group, are exploring complementary technologies, single-molecule sequencing offers the prospect of long read lengths and cost reduction, which will facilitate personalized medicine.

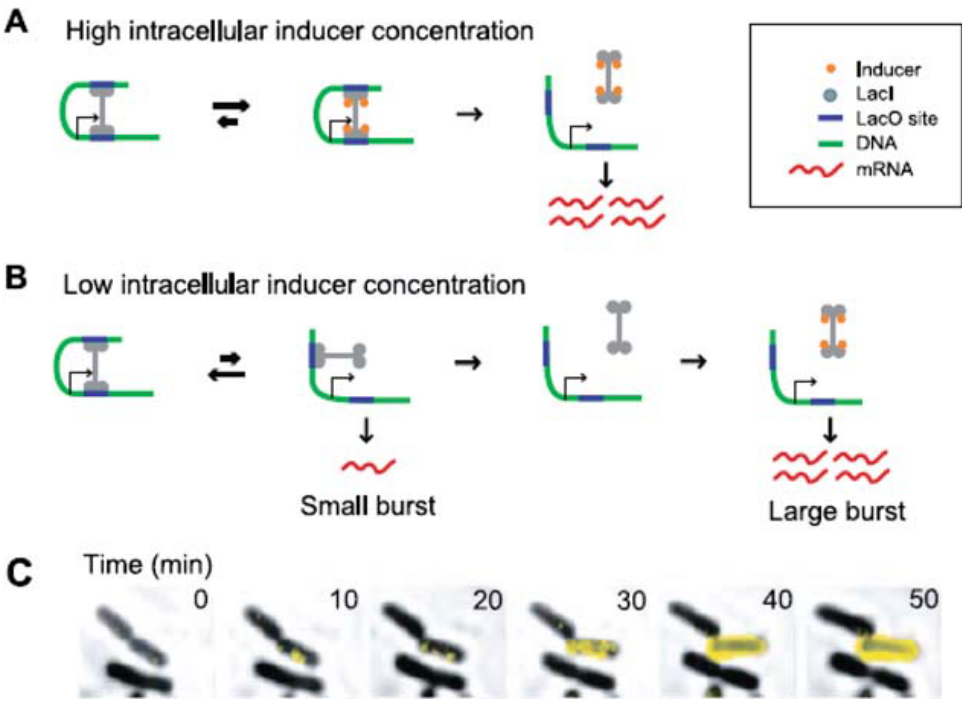

Fig. 22.8. (**A**) At high concentration of intracellular inducer, the repressor dissociates from its operators, as described by Monod and Jacob [40]. (**B**) At low concentrations of intracellular inducer, partial dissociation from one operator by the tetrameric *Lac*I repressor is followed by a fast rebinding. Consequently, no more than one transcript is generated during such a brief dissociation event. However, the tetrameric repressor can dissociate from both operators stochastically and then be sequestered by the inducer so that it cannot rebind, leading to a large burst of expression. (**C**) A time-lapse sequence captures a phenotype-switching event. In the presence of 50 mM TMG, one such cell switches phenotype to express many *Lac*Y-YFP molecules (yellow fluorescence overlay) whereas the other daughter cell does not. From ref. [41]

In our live cell work, we have chosen to study the *lac* operon, an extremely well-characterized system, in order to validate our new experimental approach, from which we have already gained new knowledge. Our goal is to apply this methodology to less well-investigated systems. To achieve this, we have constructed an *E. coli* library with each gene tagged with a yellow fluorescent protein. We have found that a large number of genes are expressed in less than a few protein molecules per cell. This further justifies why single-molecule measurements are essential. This library will serve as a basis for new discoveries.

Can single-molecule studies help medicine? I believe the answer is yes. For example, the single-molecule question regarding genetic switches as discussed above is pertinent to research on tuberculosis, a deadly bacterial disease that kills two million people each year. There is a general phenomenon in bacteria: a small population of abnormal cells, called persisters, is drug resistant.

They have the same genes as normal cells, but a drug-resistant phenotype. The biology of persisters is not understood. With the bacterial library, we are in a position to study the gene expression of persisters with single-molecule sensitivity, which could provide clues for developing drugs against tuberculosis.

In addition to bacterial research, we are attempting to conduct similar single-molecule experiments on mammalian cells, the study of which is in high demand. The question about how cells or identical genes develop different phenotypes for the *lac* operon and persisters is also pertinent to stem cells, which again emphasizes that single-molecule behaviors are important to biology.

I hope the few examples highlighted above help to illustrate that the single-molecule approach has matured as a powerful tool and offers exciting opportunities for biological discoveries. I believe the best that single-molecule science and technology can offer to biology and medicine is yet to come.

Acknowledgments

It is my pleasure to express my gratitude to current and former members of my group for their contributions summarized herein, especially Bob Dunn, Peter Lu, Haw Yang, Hongye Sun, Antoine van Oijen, Guobin Luo, Brian English, Wei Min, Ji Xiao, Ji Yu, Long Cai, Nir Friedman, Johan Elf, Gene-Wei Li, Paul Choi, Kirsten Frieda, Huiyi Chen, Yuichi Taniguchi, Peter Sims, Will Greenleaf, Sangjin Kim, Rahul Roy, and Srinjan Basu. I also acknowledge fruitful collaborations with Luying Xun, Greg Schenter, Sam Kou, Binny Cherayil, Qian Hong, Greg Verdine, Eric Rubin, Martin Karplus, Attila Szabo, Biman Bagchi and Andrew Emili. I am grateful to the DOE, NIH, NSF and the Bill and Melinda Gates Foundation for supporting our ventures.

References

1. W.E. Moerner, L. Kador, Phys. Rev. Lett. **62**, 2535–2538 (1989)
2. M. Orrit, J. Bernard, Phys. Rev. Lett. **65**, 2716–2719 (1990)
3. E. Betzig, R.J. Chichester, Science **262**, 1422–1425 (1993)
4. X.S. Xie, R.C. Duun, Science **265**, 361–364 (1994)
5. W.P. Ambrose et al., Science **265**, 364–367 (1994)
6. J.J. Macklin, J.K. Trautman, T.D. Harris, L.E. Brus, Science **272**, 255–258 (1996)
7. X.S. Xie, J.K. Trautman, Ann. Rev. Phys. Chem. **49**, 441 (1998)
8. T. Hirschfeld, Appl. Opt. **15**, 2965–2966 (1976)
9. E.B. Shera, et al., Chem. Phys. Lett. **174**, 553–557 (1990)
10. R. Rigler, J. Widengren, BioScience **3**, 180–183 (1990)
11. A. Ashkin, J.M. Dziedzic, J.E. Bjorkholm, S. Chu, Opt. Lett. **11**, 288–290 (1986)
12. S.M. Block et al., Nature **348**, 348–352 (1990)
13. S.B. Smith, Y. Cui, C. Bustamante, Science. **271**, 795–799 (1996)

14. B. Sackman, E. Neher, *Single-channel recording*, 2nd edn. (Plenum, New York and London, 1995)
15. H.P. Lu et al., Science **282**, 1877 (1998)
16. J. Yu et al., Science **311**, 1600 (2006)
17. L. Cai, N. Friedman, X.S. Xie, Nature **440**, 358 (2006)
18. R.H. Austin et al., Biochem. **14**, 5355–5373 (1975)
19. H. Yang et al., Science **302**, 262 (2003)
20. W. Min et al., Phys. Rev. Lett. **94**, 198302 (2005)
21. S. Weiss, Science **283**, 1676–1683 (1999)
22. Funatsu T et al., Nature **374**, 555 (1995)
23. M.J. Levene, J. Korlach, S.W. Turner, M. Foquet, H.G. Graighead, W.W. Webb, Science **299**, 682–686 (2003)
24. T. Ha et al., PNAS **96**, 893–898 (1999)
25. X. Zhuang et al., Science **288**, 2048–2051 (2000)
26. C. Yu, D. Hu, E.R. Vorpagel, H.P. Lu, J. Phys. Chem. B. **107**, 7947 (2003)
27. G. Luo et al., PNAS **104**, 12610–12615 (2007)
28. L. Edman et al., Chem. Phys. **247**, 11–22 (1999)
29. B. English et al., Nat. Chem. Biol. **2**, 87–94 (2006)
30. K. Velonia, O. Flomenbom, D. Loos, S. Masuo, M. Cotlet, Y. Engelborghs, J. Hofkens, A.E. Rowan, J. Klafter, R.J.M. Nolte, F.C. de Schryver, Angew. Chem. Int. Ed. (2004) **43**, 2–6 (2005)
31. L. Michaelis, M.L. Menten, Biochem. Z. **49**, 333–369 (1913)
32. W. Min et al., Nano Lett. **5**, 23773–2378 (2005)
33. W. Min, X.S. Xie, B. Bagchi, J. Phys. Chem. **112**, 454–466 (2008)
34. X.S. Xie et al., Ann. Rev. Biophys. **37**, 417–444 (2008)
35. E. Bertrand, P. Chartrand, M. Schaefer, S.M. Shenoy, R.H. Singer, R.M. Long, Mol. Cell. **2**, 437–445 (1998)
36. I. Golding, J. Paulsson, S.M. Zawilski, E.C. Cox, Cell **123**, 1026–36 (2005)
37. O.G. Berg, J. Theor. Biol. **71**, 587–603 (1975)
38. J. Elf, G. Li, X.S. Xie, Science **316**, 1191 (2007)
39. P.H. Von Hippel, O.G. Berg, J. Biol. Chem. **164**, 675–78 (1989)
40. F. Jacob, J. Monod, J. Mol. Biol. **3**, 318 (1961)
41. P. Choi, L. Cai, X.S. Xie, Science **322**, 442–446 (2008)
42. T.D. Harris et al., Science **320**, 106–109 (2008)
43. J. Eid et al., Science **323**, 133–138 (2009)